

# Effect of the elevated temperature on the local structure of lithium manganese oxide studied by in situ XAFS analysis

Youhei Shiraishi <sup>a,\*</sup>, Izumi Nakai <sup>a</sup>, Toshio Tsubata <sup>b</sup>, Takuhiro Himeda <sup>b</sup>,  
Fumishige Nishikawa <sup>b</sup>

<sup>a</sup> Department of Applied Chemistry, Faculty of Science, Science University of Tokyo, Kagurazaka, Shinjuku, Tokyo, 162 Japan

<sup>b</sup> Battery Development Laboratory, Asahi Chemical Industry, Yako, Kawasaki, Kanagawa, 210 Japan

## Abstract

Effect of the elevated temperature and that of the lithium deintercalation on the structure of stoichiometric material  $\text{LiMn}_2\text{O}_4$  and lithium excess material  $\text{Li}(\text{Mn}_{1.85}\text{Li}_{0.15})\text{O}_4$  were investigated by in situ XAFS technique. The stoichiometric material showed capacity loss after charge–discharge cycles at  $60^\circ\text{C}$  and gave deformed XAFS spectra, while the lithium excess material showed resistance to the high-temperature cycling and gave a similar XAFS spectra to the non-heated material. The XAFS analysis suggests that high-temperature cycles caused structural disorder of  $\text{LiMn}_2\text{O}_4$ , but not that of  $\text{Li}(\text{Mn}_{1.85}\text{Li}_{0.15})\text{O}_4$ . Since the lithium excess material has good structural stability against the cycling at the elevated temperature, this material will be suitable for the cathode material of the commercial batteries. © 1999 Elsevier Science S.A. All rights reserved.

**Keywords:** In situ XAFS; Lithium manganese oxide; Spinel-type structure; Local structure; Lithium ion secondary battery

## 1. Introduction

Recently, spinel lithium manganese oxide has been studied extensively as the cathode of lithium ion secondary batteries, because of the low cost of the manganese resources and its environmental advantages [1–8]. However, it is a problem of stoichiometric  $\text{LiMn}_2\text{O}_4$  that it exhibits capacity fading upon cycling. It is reported that this fading is partly attributable to the Jahn–Teller effect of the  $\text{Mn}^{3+}$  ion, whose electronic configuration is  $d^4$  [4,8,9]. Therefore, the stoichiometric  $\text{LiMn}_2\text{O}_4$  contains distorted  $\text{Mn}^{3+}$  coordination polyhedra due to the effect. The electrochemical lithium deintercalation causes oxidation of  $\text{Mn}^{3+}$  to  $\text{Mn}^{4+}$ , which is not a Jahn–Teller ion ( $d^3$ ). Thus, the charge–discharge cycling accompanies large structural change about the local structure of the Mn ions, which is responsible for the capacity fading. Moreover, it is also known that the use of the Li–Mn spinel battery at high operating temperature such as  $60^\circ\text{C}$ , which may be subjected by daily use, causes a serious capacity fading. It has been shown that adding excess lithium to the stoichiomet-

ric  $\text{LiMn}_2\text{O}_4$  reduces the capacity fading especially at elevated temperature; therefore, lithium manganese oxides with excess lithium were expected as the cathode material satisfying both good characteristics and low cost [5]. However, the mechanism of the capacity fading due to the cyclic use of the battery under elevated temperatures has not been clarified yet. XAFS technique is suitable for analyzing the behavior of the Mn atoms [10], because the manganese atoms play a major role in the redox reaction and structural change in  $\text{LiMn}_2\text{O}_4$ . Since these charge–discharge processes accompany redox reaction in transition metals that may suffer an aerial oxidation and moisture attack, it is important to obtain XAFS data without disassembling the cell. We have recently developed our original in situ transmission XAFS cell to analyze the electrochemical reaction in rechargeable lithium battery materials. The lithium deintercalation behavior of  $\text{LiNiO}_2$ ,  $\text{LiCoO}_2$ , and  $\text{LiMn}_2\text{O}_4$  has been clarified by our XAFS technique [10–12]. This method allows us to obtain XAFS data of the electrode materials at any deintercalation–intercalation stage without disassembling the cell. This paper describes the XAFS analysis of stoichiometric  $\text{LiMn}_2\text{O}_4$  and lithium-excess spinel  $\text{Li}(\text{Mn}_{1.85}\text{Li}_{0.15})\text{O}_4$  after cyclic use at an elevated temperature to reveal the effect of temperature

\* Corresponding author

on the structures of these cathode materials and variation of the structures with the lithium deintercalation.

## 2. Experimental

Stoichiometric  $\text{LiMn}_2\text{O}_4$  (sample (a)) and lithium-excess  $\text{Li}(\text{Mn}_{1.85}\text{Li}_{0.15})\text{O}_4$  (sample (b)) were prepared by a sintering method from lithium carbonate and manganese dioxide. The samples (c) and (d) were obtained by subjecting samples (a) and (b) to 20 charge–discharge cycles at  $60^\circ\text{C}$ , respectively. The samples (a), (b), (c), (d) thus prepared were assembled as the cathodes of lithium batteries in the in situ XAFS cells [10,11]. The lithium metal was used as an anode and 1 M  $\text{LiBF}_4$  in PC + EC was used as an electrolyte. The cells were subjected to the charge–discharge process for 50 min and then kept at rest for 30 min. The Mn K-edge XAFS spectra were measured by the transmission mode at various stages of the charge–discharge process. The measurements were carried out at BL-10 B, Photon Factory (PF), KEK, Japan using a Si(111) double-crystal monochromator. The REX2 [13] and FEFF 6.01 [14] computer programs were used for the analysis of the XAFS data. The back electron scattering factor and phase shift were calculated by FEFF 6.01.

## 3. Results and discussion

Fig. 1 shows the Mn K-XANES spectra of the samples as a function of the lithium deintercalation. The stoichiometric sample (a) exhibited a chemical shift of the absorption edge to higher energy side when the cell was charged, namely when the lithium atom is deintercalated. In contrast, the spectra of the heat-treated stoichiometric sample (c) are seriously deformed with suppression of their intensity and the shift of the spectra stopped soon near at  $x = 0.19$  for  $\text{Li}_{1-x}\text{Mn}_2\text{O}_4$ . The chemical shift of XANES spectrum is correlated with the oxidation state of the absorber atom, because the binding energy of an electron, which corresponds to the absorption edge energy, in the 1s orbital increases when the surrounding electrons are removed as the atom is oxidized. The steady shift of the absorption edge of the sample (a) indicates that  $\text{Mn}^{3+}$  in the spinel structure is oxidized to  $\text{Mn}^{4+}$  with the deintercalation of lithium. On the other hand, oxidation of manganese in the sample (c) does not proceed well. Moreover deformation of the spectrum and loss of the peak intensity in the sample (c) indicate that the cyclic use at the elevated temperature caused the destruction of the structure and disordering of the local structure about the manganese atoms. This observation corresponds well with the fact that

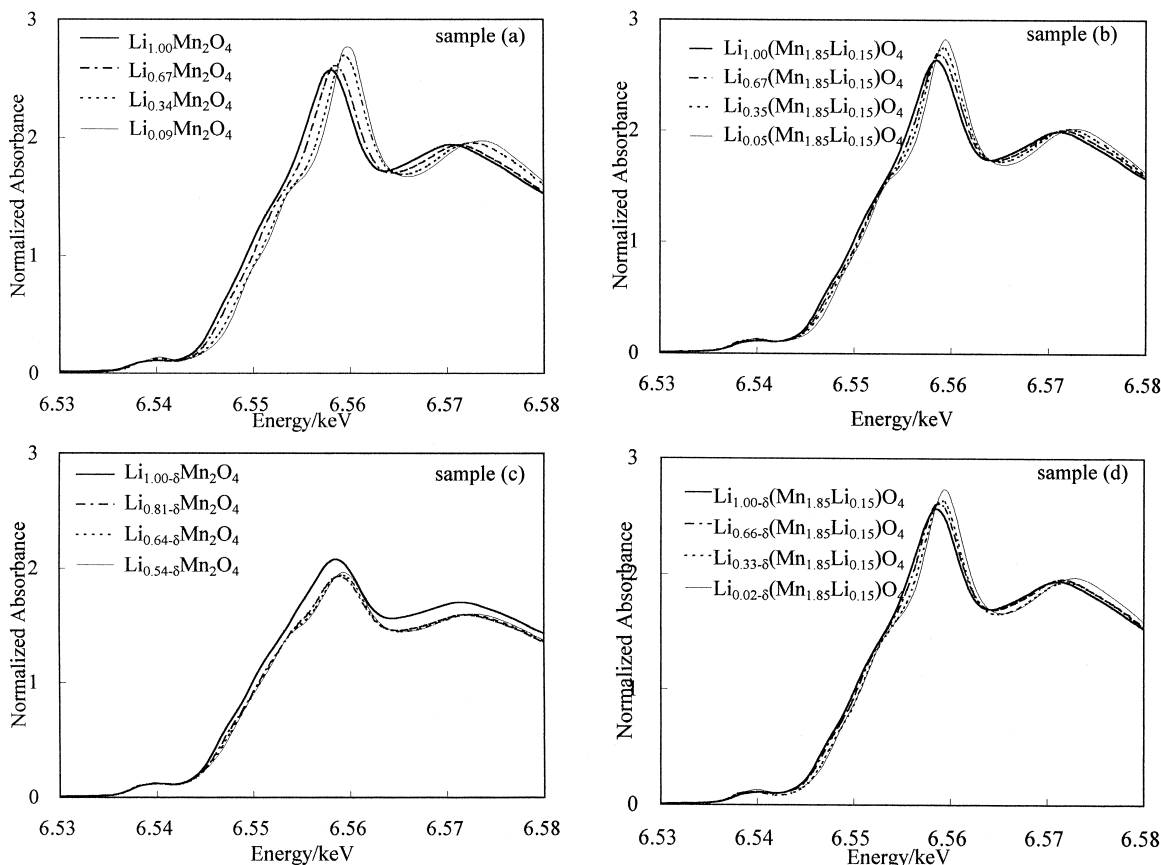


Fig. 1. Mn K-edge XANES spectra of  $\text{Li}_{1-x}\text{Mn}_2\text{O}_4$  and  $\text{Li}_{1-x}(\text{Mn}_{1.85}\text{Li}_{0.15})\text{O}_4$  measured as a function of  $x$ .

the cell with sample (c) as the cathode showed a serious capacity fading.

Fig. 2 shows the Fourier transforms (FT) of the  $k^3\chi(k)$  oscillation of the Mn K-EXAFS spectra of the samples as a function of the lithium deintercalation. The abscissa is the distance, which is not corrected for the phase shift, between the Mn atom and the coordinated atoms, and the ordinate is the Fourier transform magnitude. The first peak at around 1.5 Å in FT corresponds to the Mn–O interaction in the first coordination sphere, and the second one at around 2.5 Å is a contribution largely from the Mn–Mn interaction in the second coordination sphere, where the Mn–Li interaction is negligibly small because of the low backscattering power of the lithium atoms. At a further distance, the peak at around 4.5 Å represents the second Mn–Mn interaction, and the peak at around 5.2 Å is derived from the linear single scattering and the multiscattering caused by the manganese atom at twice the distance of the nearest manganese atom.

The sample (a) exhibited significant increase in the peak height of the FT when the cell was charged. The peak height of the FT is related to the back scattering of the photoelectron by the coordination atoms. However, when the coordination atoms are located not in uniform distance, such as a distorted octahedron with more than two Mn–O distances, the EXAFS oscillation exhibits a destructive

interference, and the apparent peak height of the FT decreases. The low peak height of the original stoichiometric sample (a) in Fig. 2 is due to the coexistence of  $\text{Mn}^{3+}$  and  $\text{Mn}^{4+}$  ions at the 16d site of the spinel structure with two different Mn–O<sub>6</sub> octahedra including the  $\text{Mn}^{3+}$  octahedron with Jahn–Teller distortion [10]. With the deintercalation of lithium,  $\text{Mn}^{3+}$  is oxidized to  $\text{Mn}^{4+}$  and the  $\text{Mn}^{4+}/\text{Mn}^{3+}$  ratio increases, and finally at  $x = 1$  for  $\text{Li}_{1-x}\text{Mn}_2\text{O}_4$ , it becomes  $\text{MnO}_2$  with a uniform  $\text{Mn}^{4+}\text{–O}_6$  octahedron. This results in an increase in the peak height of the FT. A similar tendency was observed for the 2nd peak of FT indicating an increase in the uniformity of the Mn–Mn distance with the lithium deintercalation. In contrast, the sample (c) only showed a slight increase in the peak height of these peaks when the cell was charged. This observation is consistent with the XANES result, which revealed that the cyclic use of the cell at the elevated temperature introduces disorder of the structure of the sample (c).

The enhancement of the intensity of the peak at about 5.2 Å in Fig. 2 is due to the focused multiscattering [15], which is caused by the linearity of the arrangements of the three manganese atoms. Thus, multiscattering peak is sensitive to the disorder of a crystal structure, because if three manganese atoms displace from a straight arrangement, the electron backscattering amplitude from twice the distance

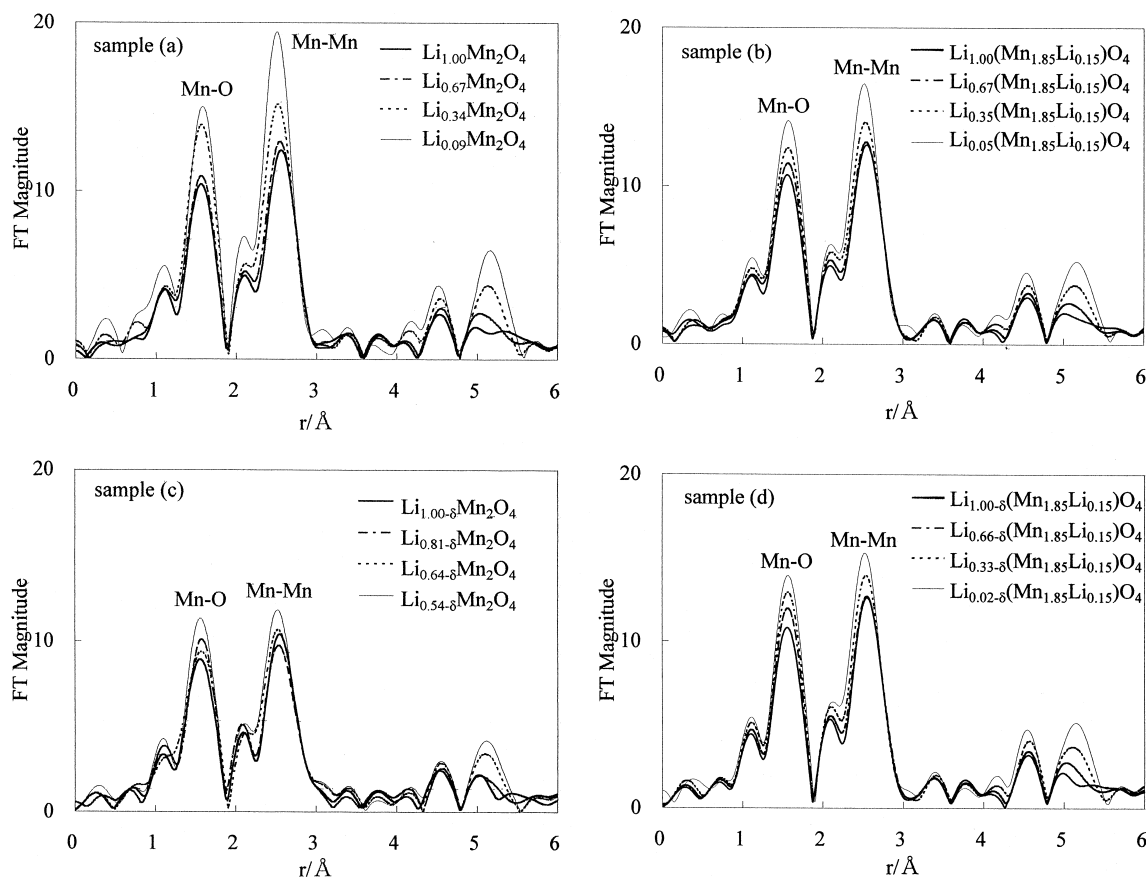


Fig. 2. Fourier transforms of  $k^3$ -weighted Mn K-edge EXAFS oscillation for  $\text{Li}_{1-x}\text{Mn}_2\text{O}_4$  and  $\text{Li}_{1-x}(\text{Mn}_{1.85}\text{Li}_{0.15})\text{O}_4$  as a function of  $x$ .

of the nearest neighbor evidently decreases. As can be seen from Fig. 2, the sample (a) shows a clear increase in the height of the multiscattering peak at around 5.2 Å, while the sample (c) only shows a small increase. This observation also confirmed that the internal structure was destroyed by the cyclic use of the cell at the elevated temperature.

Mn K-XANES spectra of the lithium excess sample  $\text{Li}(\text{Mn}_{1.85}\text{Li}_{0.15})\text{O}_4$  and that of the heat-treated sample were given in Fig. 1(b) and (d), respectively. The lithium excess sample (b) shows a similar edge shift to that of the stoichiometric sample (a) with the deintercalation of lithium, though the amount of the shift in the former sample is smaller than the latter one. This minor difference is due to the partial substitution of lithium for manganese in the sample (b), which increases the  $\text{Mn}^{4+}/\text{Mn}^{3+}$  ratio and thus reduces the capacity of the electrode. It is a marked difference between the lithium excess sample (d) and the stoichiometric sample (c) that the sample (d) also exhibits a clear chemical shift with the deintercalation of lithium even after the high-temperature cycling as seen in Fig. 1, which indicates that  $\text{Mn}^{3+}$  is oxidized normally with the deintercalation. This result is consistent with the fact that the lithium excess sample showed a good cycling performance at the elevated temperature.

A similar behavior is observed in the FT of the  $k^3\chi(k)$  oscillation of the samples (b) and (d) (Fig. 2) when the cells were charged. As can be seen from Fig. 2, the change of the pattern upon the lithium deintercalation of the sample (d) is almost the same as that of the sample (b), whose behavior is also basically equal to that of the stoichiometric sample (a); i.e., the Mn–O, Mn–Mn and multiscattering peaks all increase with the lithium deintercalation. From these observations, it is found that the lithium excess material has structural stability against the high temperature and shows good cycling performance even after the use of the cell at the elevated temperature.

#### 4. Conclusion

The present XAFS analysis has disclosed that the origin of the capacity loss of the lithium battery using stoichio-

metric manganese spinel as cathode is due to the destruction of the structure at the elevated temperature. A partial substitution of lithium for manganese in the stoichiometric spinel protects from structural fatigue at the high operating temperature. It is concluded that the structure of the lithium excess material is stable even at the elevated temperature and is suitable for the cathode material of the lithium ion secondary battery.

#### Acknowledgements

The XAFS experiments were performed with the approval of the PF program Advisory Committee (#96G182).

#### References

- [1] M.M. Thackeray, A. de Kock, W.I.F. David, *Mater. Res. Bull.* 28 (1993) 1041.
- [2] D. Guyomard, J.M. Tarascon, *Solid State Ionics* 69 (1994) 222.
- [3] R.J. Gummow, A. de Kock, M.M. Thackeray, *Solid State Ionics* 69 (1994) 59.
- [4] J.M. Tarascon, W.R. McKinnon, F. Coowar, T.N. Bowmer, G. Amatucci, D. Guyomard, *J. Electrochem. Soc.* 141 (1994) 1421.
- [5] Y. Gao, J.T. Dahn, *J. Electrochem. Soc.* 143 (1996) 1783.
- [6] N. Kumagai, T. Fujisawa, K. Tanno, *J. Electrochem. Soc.* 143 (1996) 1007.
- [7] K. Amine, H. Tukamoto, H. Yasuda, Y. Fujita, *J. Electrochem. Soc.* 143 (1996) 1607.
- [8] L. Guohua, H. Ikuta, M. Wakihara, *J. Electrochem. Soc.* 143 (1996) 178.
- [9] Y. Shimakawa, T. Numata, J. Tabuchi, *J. Solid State Chem.* 131 (1997) 138.
- [10] Y. Shiraishi, I. Nakai, T. Tsubata, T. Himeda, F. Nishikawa, *J. Solid State Chem.* 133 (1997) 587.
- [11] I. Nakai, K. Takahashi, Y. Shiraishi, T. Nakagome, F. Izumi, Y. Ishii, F. Nishikawa, T. Konishi, *J. Power Sources* 68 (1997) 536, Proceedings of IMLB 8.
- [12] I. Nakai, K. Takahashi, Y. Shiraishi, T. Nakagome, F. Nishikawa, *J. Solid State Chem.* 140 (1998) 145.
- [13] Rigaku, EXAFS analysis software, REX2, Cat. No. 2612S211, Rigaku, 1996.
- [14] S.I. Zabinsky, J.J. Rehr, A. Ankudinov, R.C. Albers, M.J. Eller, *Phys. Rev. B* 52 (1995) 2995.
- [15] P.A. O'Day, J.J. Rehr, S.I. Zabinsky, G.E. Brown Jr., *J. Am. Chem. Soc.* 116 (1994) 2938.